



Cryo-neutron crystallographic data collection and preliminary refinement of left-handed Z-DNA d(CGCGCG)

Joel M. Harp, Leighton Coates, Brendan Sullivan and Martin Egli

Acta Cryst. (2018). **F74**, 603–609



IUCr Journals

CRYSTALLOGRAPHY JOURNALS ONLINE

Copyright © International Union of Crystallography

Author(s) of this paper may load this reprint on their own web site or institutional repository provided that this cover page is retained. Republication of this article or its storage in electronic databases other than as specified above is not permitted without prior permission in writing from the IUCr.

For further information see <http://journals.iucr.org/services/authorrights.html>



Cryo-neutron crystallographic data collection and preliminary refinement of left-handed Z-DNA d(CGCGCG)

Joel M. Harp,^a Leighton Coates,^b Brendan Sullivan^b and Martin Egli^{a*}

^aDepartment of Biochemistry and Center for Structural Biology, Vanderbilt University School of Medicine, Nashville, TN 37232, USA, and ^bNeutron Scattering Division, Oak Ridge National Laboratory, 1 Bethel Valley Road, Oak Ridge, TN 37831, USA. *Correspondence e-mail: martin.egli@vanderbilt.edu

Received 15 May 2018

Accepted 24 July 2018

Edited by K. K. Kim, Sungkyunkwan University School of Medicine, Republic of Korea

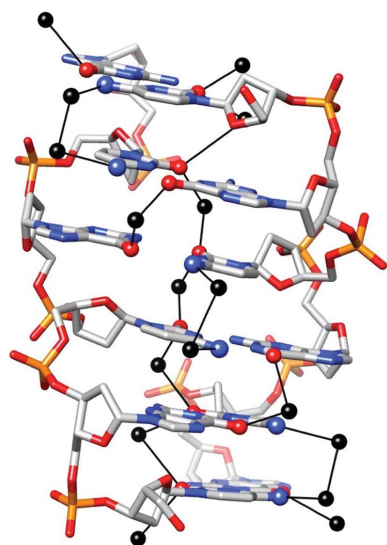
Keywords: neutron diffraction; cryogenic data collection; oligonucleotide; hydration; Z-DNA.

Supporting information: this article has supporting information at journals.iucr.org/f

Crystals of left-handed Z-DNA [d(CGCGCG)]₂ diffract X-rays to beyond 1 Å resolution, feature a small unit cell (~18 × 31 × 44 Å) and are well hydrated, with around 90 water molecules surrounding the duplex in the asymmetric unit. The duplex shows regular hydration patterns in the narrow minor groove, on the convex surface and around sugar–phosphate backbones. Therefore, Z-DNA offers an ideal case to test the benefits of low-temperature neutron diffraction data collection to potentially determine the donor–acceptor patterns of first- and second-shell water molecules. Nucleic acid fragments pose challenges for neutron crystallography because water molecules are located on the surface rather than inside sequestered spaces such as protein active sites or channels. Water molecules can be expected to display dynamic behavior, particularly in cases where water is not part of an inner shell and directly coordinated to DNA atoms. Thus, nuclear density maps based on room-temperature diffraction data with a resolution of 1.6 Å did not allow an unequivocal determination of the orientations of water molecules. Here, cryo-neutron diffraction data collection for a Z-DNA crystal on the Macromolecular Neutron Diffractometer at the Spallation Neutron Source at Oak Ridge National Laboratory and the outcome of an initial refinement of the structure are reported. A total of 12 diffraction images were recorded with an exposure time of 3.5 h per image, whereby the crystal was static for each diffraction image with a 10° φ rotation between images. Initial refinements using these neutron data indicated the positions and orientations of 30 water molecules within the first hydration shell of the DNA molecule. This experiment constitutes a state-of-the-art approach and is the first attempt to our knowledge to determine the low-temperature neutron structure of a DNA crystal.

1. Introduction

The DNA hexamer d(CGCGCG) was the first oligonucleotide for which a single-crystal X-ray structure was reported (Wang *et al.*, 1979). At the time of its publication almost 40 years ago, this Z-DNA structure caused somewhat of a shock as the two antiparallel strands were wound around each other in a left-handed fashion. Thus, Z-DNA bore little resemblance to the model of the right-handed double helix built by Watson and Crick (Watson & Crick, 1953). The striking features of Z-DNA include the zigzag-like (hence Z-DNA) arrangement of phosphate groups along the backbones (Fig. 1), alternating low (−10°; CpG steps) and high (−50°; GpC steps) helical twists, different sugar puckers adopted by cytosines (C2'-*endo*) and guanines (C3'-*endo*), and a convex surface in place of the major groove. In Z-DNA crystals duplexes are tightly packed, resulting in a small volume per base pair of ~1000 Å³. Z-DNA crystals diffract X-rays to an exceptionally high resolution of beyond 0.6 Å (Tereshko *et al.*, 2001), permitting visualization



© 2018 International Union of Crystallography

of virtually all of the waters in the asymmetric unit (~ 85 ; Gessner *et al.*, 1994). Thus, the structures of Z-DNA crystals grown under various conditions (pure Mg^{2+} form, pure spermine form, mixed spermine/ Mg^{2+} form *etc.*) have revealed intricate patterns of hydration (i) in the narrow minor groove [with water molecules bridging adjacent O2(C) atoms from opposite strands; Fig. 1]; (ii) across and along strands on the convex surface [for example, water molecules bridging N4(C) pairs and O6(G) pairs from opposite strands; Fig. 1]; and (iii) linking phosphates and base donor/acceptor atoms (Gessner *et al.*, 1994). The low-temperature X-ray structure of the pure spermine form of Z-DNA also showed a spermine molecule winding down the minor groove, thereby locally displacing water molecules from the spine (Bancroft *et al.*, 1994).

Although X-ray crystal structures at or near atomic resolution can convey a detailed picture of the water structure that surrounds oligonucleotides (Gessner *et al.*, 1994; Egli *et al.*, 1996, 2000), such structures, even those at an ultrahigh resolution of 0.6 Å (Tereshko *et al.*, 2001), are typically blind to the positions of H atoms of solvent molecules. Neutron macromolecular crystallography (NMC) allows one to visualize H (D) atoms in the structures of proteins and nucleic acids, as shown by recent successes in the application of this approach (Leal *et al.*, 2010; Fenn *et al.*, 2011; Chen *et al.*, 2012; Cuyper *et al.*, 2013). Thus, Niimura and coworkers reported the first NMC structures of DNA fragments: a left-handed Z-DNA hexamer (Chatake *et al.*, 2005) and a B-DNA decamer (Arai *et al.*, 2005). In the Z-DNA neutron structure at 1.80 Å resolution, 44 water molecules, representing about 50% of the solvent content of the asymmetric unit of the orthorhombic Z-DNA crystals, were included in the refinement. Perhaps as a

result of the limited resolution and the considerable number of missing reflections (74% overall completeness, 41% in the outer shell), the nuclear density allowed only a tentative assignment of deuterium peaks and therefore was of insufficient quality to settle the orientations of many water molecules. Although the positions of D atoms present in the nucleobases are readily visible in nuclear density maps at resolutions of around 1.6 Å (Fig. 2, our unpublished data), water molecules exhibit higher mobility than DNA atoms and room-temperature data are therefore unlikely to ever produce a meaningful model of the hydration surrounding a nucleic acid fragment. We hypothesized that a neutron structure of Z-DNA based on data collected at low temperature might eventually produce an improved model of the orientations of first-shell and perhaps also second-shell water molecules around the duplex.

Owing to the fact that neutrons do not induce radiation damage, the use of cryocooling in NMC has been limited. However, the ability to freeze-trap or reduce the mobility of interacting water molecules is a key benefit of cryocooling. Concanavalin A is a well studied lectin which binds to different saccharides. A detailed comparison between two neutron structures collected at room temperature (Habash *et al.*, 2000) and at 15 K (Blakeley *et al.*, 2004) showed that twice as many water molecules could be located in the structure at 15 K. Additionally, the atomic displacement parameters for the water molecules were reduced by around fourfold in the 15 K structure compared with the room-temperature structure. Thus, it seems likely that collecting a neutron diffraction data set from a cryocooled Z-DNA crystal should enable the observation of more water molecules present in the

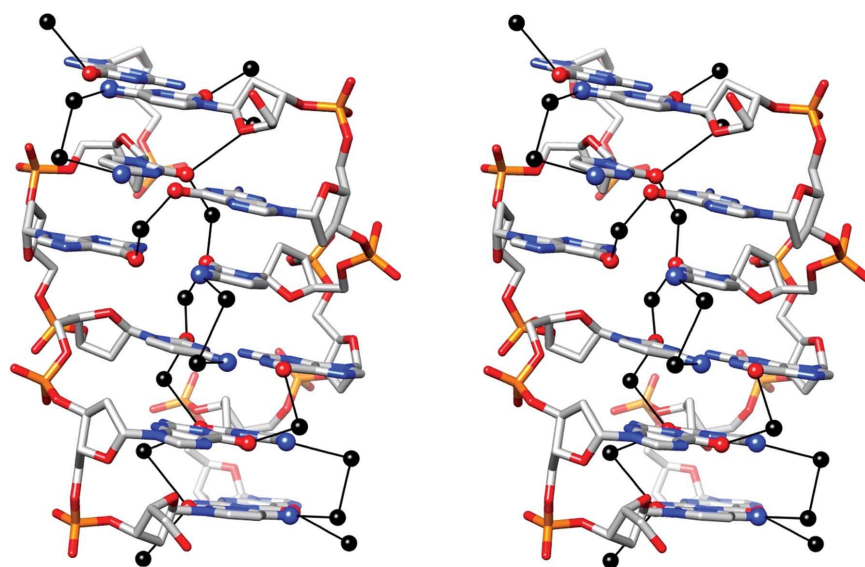


Figure 1

Cross-eyed stereoview of repetitive hydration patterns involving nucleobase atoms on the convex surface (the equivalent of the major groove in Z-DNA) and in the minor groove of the Z-DNA hexamer seen in the X-ray crystal structure of the so-called Mg^{2+} form (four Mg^{2+} ions; PDB entry 1dgg; Gessner *et al.*, 1989) at 1 Å resolution. Water-molecule tandems link N4 atoms from adjacent C pairs across strands on the convex surface. Also on the convex surface, a single water links O6 atoms from adjacent G pairs that belong to opposite strands. Inside the minor groove, single water molecules link O2 atoms from adjacent cytosines, thus generating a spine of hydration visible as a zigzag-shaped line in the background that connects alternating O2 atoms and waters. Water molecules are shown as black spheres, hydrogen bonds are shown as solid lines and O6(G), N4(C) and O2(C) atoms are highlighted as spheres colored red (O) and blue (N).

asymmetric unit than would be revealed at room temperature. More recently, cryocooling has been used in NMC to study transient protein–ligand complexes in β -lactamases (Coates *et al.*, 2014) and to investigate protonation states in cytochrome *c* peroxidase, revealing that the ferryl heme in compound I is

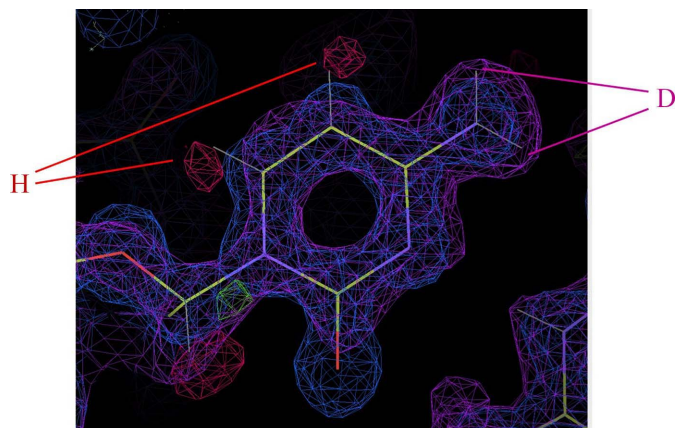


Figure 2
Nuclear (purple) and electron (blue) density around a Z-DNA cytosine base based on a joint X-ray/neutron refinement using room-temperature data to 1.1 and 1.6 Å resolution, respectively. The positions of D and H atoms are marked.

unprotonated and resolving a decades-old debate (Casadei *et al.*, 2014).

Here, we report cryo-neutron diffraction data collection for a Z-DNA hexamer crystal with an approximate volume of 0.25 mm³. Data were collected at 100 K on the Macromolecular Neutron Diffractometer (MaNDi; Coates *et al.*, 2015) at the Spallation Neutron Source (SNS), Oak Ridge National Laboratory (ORNL), Oak Ridge, Tennessee, USA in less than 2 d and are 91% complete to a resolution of 1.7 Å.

2. Materials and methods

2.1. Crystallization experiments

The Z-DNA hexamer d(CGCGCG) was synthesized and HPLC-purified by Integrated DNA Technologies. Lyophilized DNA hexamer was dissolved in D₂O to a concentration of 50 mg ml⁻¹. Crystals were grown without spermine according to the method of Langan *et al.* (2006). The crystallization buffer was prepared using dry MES, ammonium sulfate and magnesium acetate dissolved in D₂O to give 2.5 M ammonium sulfate, 10 mM magnesium acetate, 50 mM MES. The final pH of the buffer was 6.1. Crystals were grown by mixing equal volumes of DNA solution and crystallization buffer and

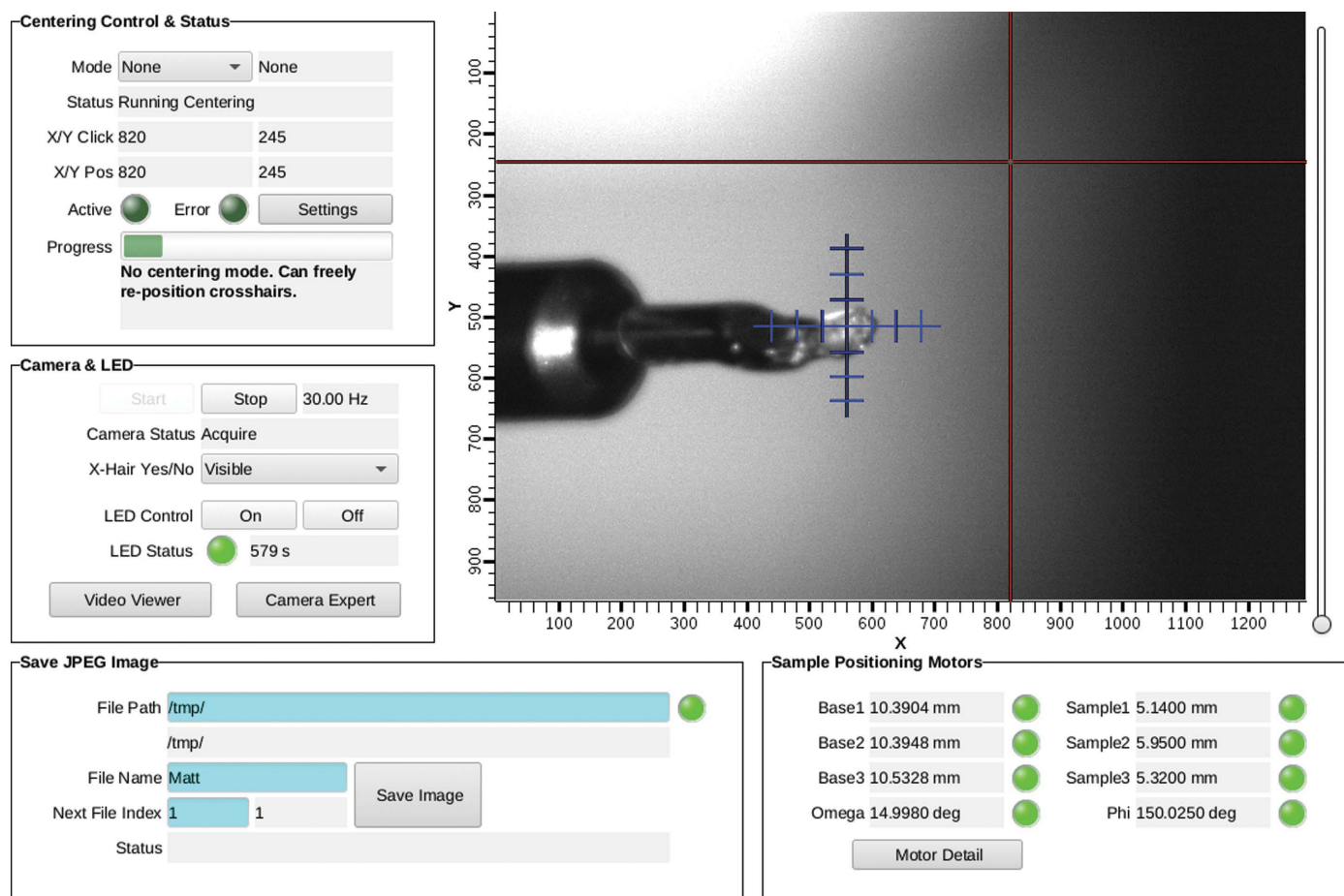


Figure 3
The Z-DNA crystal mounted on the MaNDi goniostat is ready to be centered. No ice accumulation was observed over the 2 d of data collection.

Table 1
Data-collection and processing statistics.

Space group	<i>P</i> 2 ₁ 2 ₁ 2 ₁
<i>a</i> , <i>b</i> , <i>c</i> (Å)	17.89, 30.77, 43.71
α , β , γ (°)	90, 90, 90
Resolution range (Å)	10.30–1.70 (2.00–1.70)
Total No. of reflections	9386 (519)
No. of unique reflections	2648 (232)
Completeness (%)	91.37 (82.56)
Multiplicity	3.54 (2.24)
$\langle I/\sigma(I) \rangle$	8.6 (3.0)
R_{merge} (%)	15.8 (23.0)
$R_{\text{p.i.m.}}$ (%)	8.0 (15.2)
$CC_{1/2}$ (%)	98.0 (91.9)

equilibrating the drops by vapor diffusion against a reservoir of crystallization buffer. Crystals were cryoprotected by immersion in Paratone-N oil to remove excess mother liquor and then removing all but a thin layer of oil from the surface of the crystal. The crystal was then mounted on a 600 μm MiTeGen dual-thickness micromount and was flash-cooled by plunging into liquid nitrogen. The crystal was stored in liquid nitrogen and transported to the SNS.

2.2. Neutron diffraction data collection and processing

The collection of neutron diffraction data often requires the sample to be kept at 100 K for extended periods of time (2–18 d) without the formation of ice on the sample. To help to reduce the likelihood of ice formation on the sample, several modifications were made to the MaNDi goniometer. Most notably, the goniometer χ angle was altered from 135 to 45° as this changes the angle at which the sample pin enters the cryostream, reducing the formation of ice on the sample pin (Fig. 3), which can eventually work its way onto the sample. The goniostat and cryostat assembly with a mounted crystal

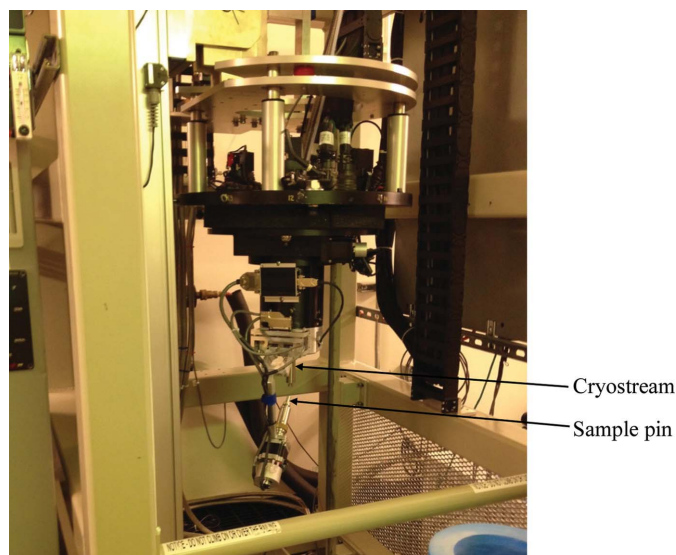


Figure 4
An image of the Z-DNA crystal mounted on a sample pin on the MaNDi goniostat and in the cryostream maintained at 100 K. The entire assembly is lowered into the detector sphere in preparation for cryogenic neutron diffraction data collection.

ready to be lowered into the spherical detector array is shown in Fig. 4. Data were collected using position- and time-sensitive SNS Anger cameras with each individual event being stored. To collect a complete data set at 100 K on the MaNDi instrument (Coates *et al.*, 2015), 12 diffraction images were collected with an exposure time of 3.5 h each. The crystal was held static during each diffraction image and was rotated 10° in φ between images. Data collection was completed in 42 h, yielding a complete data set to a resolution of 1.70 Å (Table 1). These data were converted to histograms in reciprocal space using the *Mantid* program (Arnold *et al.*, 2014) and integrated using profile fitting. Briefly, the three-dimensional intensity profile of each peak is fitted as the product of a bivariate Gaussian and an Ikeda–Carpenter function; weak peaks are fitted by assuming the profile of a nearby strong peak and scaling the profile to match the data. Integrated intensities were then scaled using *LAUENORM* from the *LAUEGEN* suite (Campbell *et al.*, 1998). The reduced and corrected data statistics are shown in Table 2.

2.3. Refinement

Initial phases were obtained by the molecular-replacement technique using the high-resolution model of the Z-DNA duplex based on the X-ray structure of crystals grown under identical conditions (PDB entry 3qba; Fenn *et al.*, 2011). All crystallographic refinements were carried out with *PHENIX* (Adams *et al.*, 2010) and model building was performed using the *Coot* molecular-graphics program (Emsley *et al.*, 2010).

3. Results and discussion

The crystal form of the Z-DNA hexamer analyzed here is identical to that first described by Langan *et al.* (2006), who relied on ammonium sulfate as the precipitant instead of the more commonly used 2-methyl-2,4-pentanediol (MPD) or 2-propanol. Also noteworthy is the absence of spermine when growing the crystals, which precludes the disturbance of the water structure around the left-handed duplex by polyamines associated with the convex surface (Gessner *et al.*, 1994) or the minor groove (Bancroft *et al.*, 1994). Unlike Langan and coworkers, who grew large crystals of the ammonium sulfate form directly in a capillary and then exchanged the hydrogenous mother liquor for the D₂O equivalent including (ND₄)₂SO₄ for data collection at room temperature, we obtained crystals by the sitting-drop vapor-diffusion technique directly in D₂O solution. However, we did not use the perdeuterated form of ammonium sulfate. The concentration of the latter is 2.5 M in the reservoir, and this is likely to be the reason why the H atoms at exocyclic amino groups of some cytosines (N4) and guanines (N2) as well as the H atoms at N1 of guanine were only partially exchanged for deuterium, as shown by the nuclear density around guanine and cytosine nucleobases (Fig. 5). On the other hand, a 5'-terminal hydroxyl group appears to be fully deuterated (Fig. 6)

Neutron crystallography has been hampered by the more difficult access to beamlines compared with routine data

Table 2
Data statistics.

Resolution (Å)	No. of observations	No. of unique observations	Multiplicity	Completeness (%)	$\langle I \rangle$	$\langle I/\sigma(I) \rangle$	R_{merge}	$R_{\text{p.i.m.}}$	$CC_{1/2}$
10.58–3.62	982	272	3.61	85.27	709.6	22.7	0.148	0.077	0.949
3.62–2.89	1321	299	4.42	97.71	475.7	19.6	0.119	0.056	0.983
2.89–2.53	1213	277	4.38	95.85	140.0	9.7	0.181	0.088	0.920
2.53–2.30	1188	275	4.32	95.16	92.3	7.4	0.206	0.100	0.911
2.30–2.14	1036	273	3.79	94.79	62.8	5.3	0.243	0.124	0.883
2.14–2.01	973	272	3.58	97.49	49.6	4.3	0.256	0.137	0.801
2.01–1.91	872	267	3.27	91.13	50.5	4.1	0.272	0.152	0.742
1.91–1.83	688	251	2.74	92.62	46.7	3.5	0.246	0.146	0.783
1.83–1.76	594	230	2.58	82.14	43.1	3.1	0.252	0.160	0.861
1.76–1.70	519	232	2.24	82.56	48.2	3.0	0.230	0.152	0.919
10.58–1.70	9386	2648	3.54	91.37	179.9	8.6	0.158	0.080	0.980

collections at X-ray synchrotrons and the need for large crystals as well as long exposure times that in the past

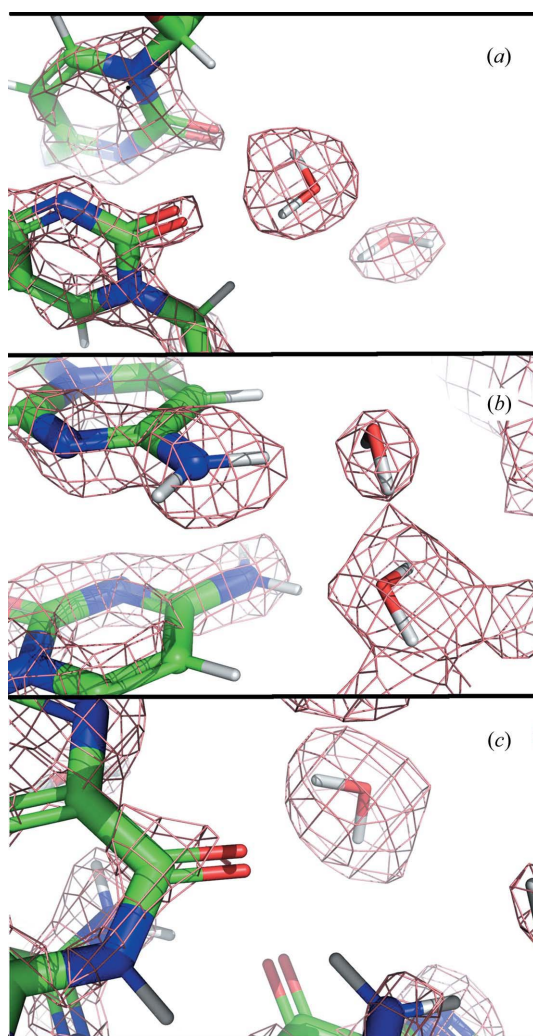


Figure 5
Examples of nuclear density for waters in a preliminary structure of Z-DNA using data to 1.7 Å resolution collected at 100 K. (a) A single water bridging the O2 atoms of cytosines on opposite strands. (b) Two waters bridging the N4 atoms of cytosines on opposite strands. (c) A single water bridging the O6 atoms of guanosines on opposite strands. All density was contoured at 1.5 r.m.s.d. This figure was prepared using *PyMOL* v.2.0 (Schrödinger).

frequently required several weeks without resulting in high overall data completeness (a process now reduced to mere minutes using X-rays of high brilliance and fast detectors in combination with the shutterless mode of operation). Although the Z-DNA crystal used for data collection here was less than 0.25 mm³ in size, we obtained a data set of high completeness to a maximum resolution of 1.7 Å. Thus, the MaNDi/SNS setup lives up to its promise of enabling neutron diffraction experiments with smaller crystals. The Z-DNA crystal used by Langan and coworkers for data collection at the Protein Crystallography Station (PCS) at Los Alamos National Laboratory (Chen & Unkefer, 2017) was almost three times the volume (0.7 mm³) of the crystal used at MaNDi. Data collection at the PCS took a total of around 21 d, compared with less than 2 d on MaNDi. Thus, data collection on MaNDi is over an order of magnitude faster than using the previous generation of neutron protein crystallography instrumentation. This is owing in part to the large area-detector coverage on the MaNDi instrument (Coates *et al.*, 2015) and the increased neutron flux available at the SNS.

The fact that data were obtained in less than 2 d raises the prospect of data acquisition for several crystals per week. Another innovative feature of our experiment is data collection at low temperature. Although crystals do not suffer damage from exposure to neutrons, even when in the beam for extended periods of time, cryo-neutron diffraction experiments still offer some advantages. In particular, higher quality

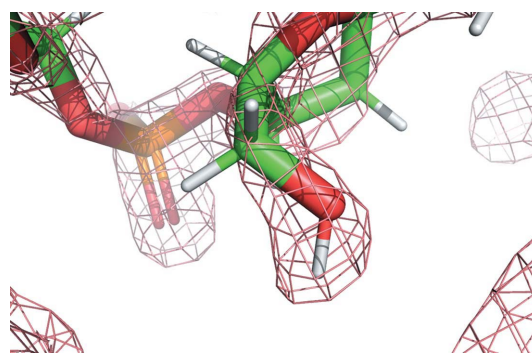


Figure 6
A nuclear density map indicating deuterium exchange on the terminal 5'-hydroxyl group. Density was contoured at 1.5 r.m.s.d. This figure was prepared using *PyMOL* v.2.0 (Schrödinger).

data is anticipated in dynamic structural regions such as flexible portions of a macromolecule or, as demonstrated here, in identifying water molecules that are not situated inside the grooves of a DNA duplex. In the case of an enzyme active site or an ion channel, low-temperature data collection may pave the way to resolving dynamic disorder, allowing better determination of the orientations of D_2O molecules.

The benefits of low-temperature data collection for accurately visualizing solvent molecules in Z-DNA crystals have previously been demonstrated with the structure of the pure spermine form of the left-handed hexamer duplex. Both room-temperature (Egli *et al.*, 1991) and low-temperature (Bancroft *et al.*, 1994) structures were determined to a resolution of 1 Å. However, in the latter 15 additional water molecules per asymmetric unit were identified as well as a second spermine molecule that was bound in the narrow minor groove. Moreover, the water molecules in the low-temperature structure exhibited drastically reduced temperature factors on average compared with the structure based on data collected at room temperature (Fig. 7). Therefore, in order to successfully resolve the orientations of as many water molecules as possible in nuclear density maps, low-temperature data collection is a must. This conclusion is further supported by a comparison of the temperature factors of protein atoms in the recently analyzed room-temperature and low-temperature neutron crystal structures of β -lactamase (see Fig. 5 in Coates *et al.*, 2014).

In the initial stages of refinement, we included 30 solvent molecules that mostly belong to the first hydration shell. It is noteworthy that the numbers of water molecules in X-ray and neutron crystal structures of comparable resolution differ considerably. For example, the X-ray structure of the Z-DNA duplex at a resolution of 1.5 Å features 56 water molecules. The corresponding neutron structure at 1.8 Å resolution contains only 37 water molecules (Chatake *et al.*, 2005). Even

in the jointly refined X-ray/neutron crystal structure of the Z-DNA hexamer at 1.5 Å resolution, just 41 water molecules were assigned to density maps (Fenn *et al.*, 2011). These account for less than half of the waters observed in the same crystallographic asymmetric unit of Z-DNA crystal structures at atomic resolution (Gessner *et al.*, 1994). It is unclear why it would be easier to visualize water molecules in electron-density maps than in nuclear density maps drawn at a resolution of around 1.5 Å. After all, the coherent neutron scattering lengths of deuterium and oxygen are quite similar (6.7 and 5.8 fm, respectively), whereas X-rays are basically blind to H atoms at medium resolution. Still, the preliminary analysis of the distribution of water molecules in our low-temperature neutron structure is quite encouraging. In the minor groove, a single water acts as a donor in two hydrogen bonds to O2 keto oxygens of cytosines from opposite strands (Fig. 5a). The nuclear density also reveals a plausible hydrogen-bonding pattern for tandem waters linking N4 amino groups from adjacent cytosines on the convex surface (Fig. 5b). Similar to the orientation of the water molecule bridging neighboring cytosines in the minor groove, water donates hydrogen bonds to O6 keto oxygens from adjacent guanines on the convex surface (Fig. 5c).

Despite these insights, it is clear that nuclear density at 1.7 Å resolution, even based on diffraction data collected at low temperature, is not sufficient to settle the orientations of all first-shell and second-shell water molecules around the Z-DNA duplex. Therefore, to visualize more or ultimately all water molecules, *i.e.* as many as 85, representing the entire water content of the asymmetric unit in the orthorhombic form of the hexamer, it will be necessary to extend the resolution of the nuclear density to 1 Å or higher. While the MaNDi/SNS setup currently represents the state of the art with regard to neutron flux and detector technology, such an experiment will require larger crystals and longer exposures per frame. Crystals of the ammonium sulfate form of Z-DNA with an approximate volume of 1 mm³ can be grown (Fig. 8) and, provided that the flash-cooling of a cryoprotected large specimen can be achieved without causing damage, we believe

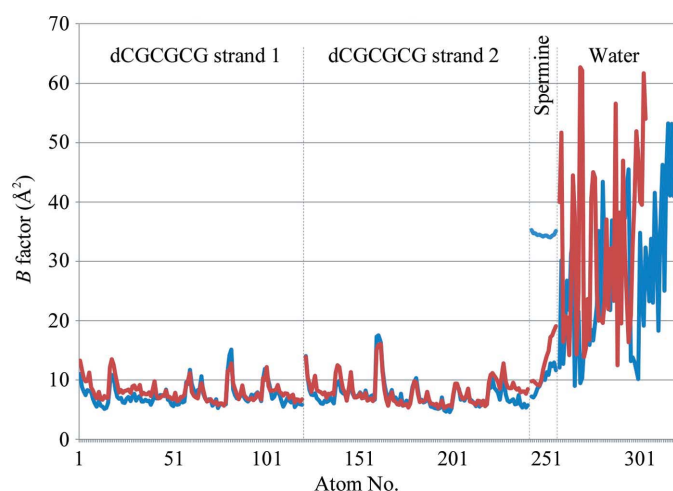


Figure 7
Comparison of temperature factors and numbers of solvent molecules in the structures of the pure spermine form of Z-DNA determined at room temperature (Egli *et al.*, 1991; PDB entry 1d48; red) and low temperature (Bancroft *et al.*, 1994; PDB entry 131d; blue) demonstrates the benefits of cryogenic data collection.

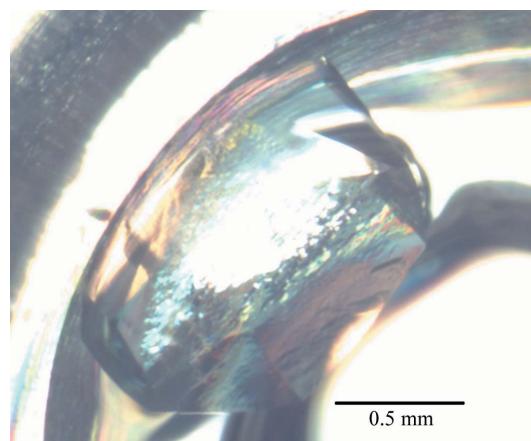


Figure 8
An ammonium sulfate form crystal of Z-DNA with an approximate volume of 1 mm³.

that low-temperature data collection for about a week might furnish a data set of high completeness to atomic resolution. We intend to collect such data in the near future in order to establish a more definitive experimental model of the water structure around a DNA duplex.

Funding information

The research at ORNL's Spallation Neutron Source was sponsored by the Scientific User Facilities Division, Office of Basic Energy Sciences, US Department of Energy. This work was also supported in part through grant R01-GM071939 from the National Institutes of Health.

References

- Adams, P. D. *et al.* (2010). *Acta Cryst.* **D66**, 213–221.
- Arai, S., Chatake, T., Ohhara, T., Kurihara, K., Tanaka, I., Suzuki, N., Fujimoto, Z., Mizuno, H. & Niimura, N. (2005). *Nucleic Acids Res.* **33**, 3017–3024.
- Arnold, O. *et al.* (2014). *Nucl. Instrum. Methods Phys. Res. A*, **764**, 156–166.
- Bancroft, D., Williams, L. D., Rich, A. & Egli, M. (1994). *Biochemistry*, **33**, 1073–1086.
- Blakeley, M. P., Kalb, A. J., Helliwell, J. R. & Myles, D. A. A. (2004). *Proc. Natl Acad. Sci. USA*, **101**, 16405–16410.
- Campbell, J. W., Hao, Q., Harding, M. M., Nguti, N. D. & Wilkinson, C. (1998). *J. Appl. Cryst.* **31**, 496–502.
- Casadei, C. M., Gumiero, A., Metcalfe, C. L., Murphy, E. J., Basran, J., Concilio, M. G., Teixeira, S. C. M., Schrader, T. E., Fielding, A. J., Ostermann, A., Blakeley, M. P., Raven, E. L. & Moody, P. C. E. (2014). *Science*, **345**, 193–197.
- Chatake, T., Tanaka, I., Umino, H., Arai, S. & Niimura, N. (2005). *Acta Cryst.* **D61**, 1088–1098.
- Chen, J. C.-H., Hanson, L., Fisher, S. C., Langan, P. & Kovalevsky, A. Y. (2012). *Proc. Natl Acad. Sci. USA*, **109**, 15301–15306.
- Chen, J. C.-H. & Unkefer, C. J. (2017). *IUCrJ*, **4**, 72–86.
- Coates, L., Cuneo, M. J., Frost, M. J., He, J., Weiss, K. L., Tomanicek, S. J., McFeeters, H., Vandavasi, V. G., Langan, P. & Iverson, E. B. (2015). *J. Appl. Cryst.* **48**, 1302–1306.
- Coates, L., Tomanicek, S., Schrader, T. E., Weiss, K. L., Ng, J. D., Jüttner, P. & Ostermann, A. (2014). *J. Appl. Cryst.* **47**, 1431–1434.
- Cuyppers, M. G., Mason, S. A., Blakeley, M. P., Mitchell, E. P., Haertlein, M. & Forsyth, V. T. (2013). *Angew. Chem. Int. Ed.* **52**, 1022–1025.
- Egli, M., Portmann, S. & Usman, N. (1996). *Biochemistry*, **35**, 8489–8494.
- Egli, M., Tereshko, V., Teplova, M., Minasov, G., Joachimiak, A., Sanishvili, R., Weeks, C. M., Miller, R., Maier, M. A., An, H., Cook, P. D. & Manoharan, M. (2000). *Biopolymers*, **48**, 234–252.
- Egli, M., Williams, L. D., Gao, Q. & Rich, A. (1991). *Biochemistry*, **30**, 11388–11402.
- Emsley, P., Lohkamp, B., Scott, W. G. & Cowtan, K. (2010). *Acta Cryst.* **D66**, 486–501.
- Fenn, T. D., Schnieders, M. J., Mustyakimov, M., Wu, C., Langan, P., Pande, V. S. & Brunger, A. T. (2011). *Structure*, **19**, 523–533.
- Gessner, R. V., Frederick, C. A., Quigley, G. J., Rich, A. & Wang, A. H.-J. (1989). *J. Biol. Chem.* **264**, 7921–7935.
- Gessner, R. V., Quigley, G. J. & Egli, M. (1994). *J. Mol. Biol.* **236**, 1154–1168.
- Habash, J., Raftery, J., Nuttall, R., Price, H. J., Wilkinson, C., Kalb (Gilboa), A. J. & Helliwell, J. R. (2000). *Acta Cryst.* **D56**, 541–550.
- Langan, P., Li, X., Hanson, B. L., Coates, L. & Mustyakimov, M. (2006). *Acta Cryst.* **F62**, 453–456.
- Leal, R. M. F., Callow, S., Callow, P., Blakeley, M. P., Cardin, C. J., Denny, W. A., Teixeira, S. C. M., Mitchell, E. P. & Forsyth, V. T. (2010). *Acta Cryst.* **D66**, 1244–1248.
- Tereshko, V., Wilds, C. J., Minasov, G., Prakash, T. P., Maier, M. A., Howard, A., Wawrzak, Z., Manoharan, M. & Egli, M. (2001). *Nucleic Acids Res.* **29**, 1208–1215.
- Wang, A. H.-J., Quigley, G. J., Kolpak, F. J., Crawford, J. L., van Boom, J. H., van der Marel, G. A. & Rich, A. (1979). *Nature (London)*, **282**, 680–686.
- Watson, J. D. & Crick, F. H. C. (1953). *Nature (London)*, **171**, 737–738.